Title
mTORC1 inhibition delays growth of neurofibromatosis type 2 schwannoma

Journal
Neuro-Oncology, 16(4)

ISSN
1522-8517

Authors
Giovannini, Marco
Bonne, Nicolas-Xavier
Vitte, Jeremie
et al.

Publication Date
2014-04-01

DOI
10.1093/neuonc/not242

Peer reviewed

Neuro-Oncology

Neuro-Oncology 16(4), 493–504, 2014
doi:10.1093/neuonc/not242
Advance Access date 10 January 2014

mTORC1 inhibition delays growth of neurofibromatosis type 2 schwannoma

Marco Giovannini, Nicolas-Xavier Bonne†, Jeremie Vitte†, Fabrice Chareyre, Karo Tanaka, Rocky Adams, Laurel M. Fisher, Laurence Valeyrie-Allanore, Pierre Wolkenstein, Stephane Goutagny, and Michel Kalamarides

House Research Institute, Center for Neural Tumor Research, Los Angeles, CA, USA (M.G., N.-X.B., J.V., F.C., K.T., R.A., L.M.F.); Department of Cell and Neurobiology, University of Southern California, Keck School of Medicine, Los Angeles, California (M.G.); Département de Dermatologie, Centre de référence des neurofibromatoses, Hôpital Henri-Mondor, AP-HP and EA 4393 LIC, Université Paris Est Créteil, Créteil, France (L.V.-A., P.W.); Department of Neurosurgery, AP-HP, Hopital Beaujon, Clichy, France (S.G); Department of Neurosurgery, AP-HP, Hôpital Pitié Salpêtrière, Paris Cedex 13, France (M.K.); Université Pierre et Marie Curie, Faculté de Médecine, Paris Cedex 13, France (M.K.); Unité Inserm U674, Fondation Jean Dausset, Paris, France (S.G., M.K.)

Corresponding Authors: Marco Giovannini, MD, PhD, Department of Head and Neck Surgery, David Geffen School of Medicine at UCLA, 10833 Le Conte Ave, Los Angeles, CA 90095-1624 (mgiovannini@mednet.ucla.edu); Michel Kalamarides, MD, PhD, Department of Neurosurgery, Hôpital Pitié Salpêtrière, Assistance Publique-Hôpitaux de Paris, 47-83 Bd. de l'Hôpital, 75651 Paris Cedex 13, France (michel.kalamarides@psl.aphp.fr).
†These authors contributed equally to this work.

See the editorial by Plotkin, on pages 471–472.

Background. Neurofibromatosis type 2 (NF2) is a rare autosomal dominant genetic disorder, resulting in a variety of neural tumors, with bilateral vestibular schwannomas as the most frequent manifestation. Recently, merlin, the NF2 tumor suppressor, has been identified as a novel negative regulator of mammalian target of rapamycin complex 1 (mTORC1); functional loss of merlin was shown to result in elevated mTORC1 signaling in NF2-related tumors. Thus, mTORC1 pathway inhibition may be a useful targeted therapeutic approach.

Methods. We studied in vitro cell models, cohorts of mice allografted with $Nf2^{-/-}$ Schwann cells, and a genetically modified mouse model of NF2 schwannoma in order to evaluate the efficacy of the proposed targeted therapy for NF2.

Results. We found that treatment with the mTORC1 inhibitor rapamycin reduced the severity of NF2-related Schwann cell tumorigenesis without significant toxicity. Consistent with these results, in an NF2 patient with growing vestibular schwannomas, the rapalog sirolimus induced tumor growth arrest.

Conclusions. Taken together, these results constitute definitive evidence that justifies proceeding with clinical trials using mTORC1-targeted agents in selected patients with NF2 and in patients with NF2-related sporadic tumors.

Keywords: neurofibromatosis type 2, rapamycin, schwannoma.

Schwannomas are common benign tumors originating from Schwann cells of peripheral or cranial nerves. Vestibular schwannomas (VSs), previously known as acoustic neuromas, develop late in life and account for 9% of intracranial tumors in humans.[1] By contrast, patients with the tumor predisposition syndrome neurofibromatosis type 2 (NF2) develop multiple schwannomas early in life, including bilateral VS, the hallmark of the disease.[2] The intractable location of these tumors renders treatment difficult; the primary treatment modality is surgical resection or, increasingly, radiosurgery, with the associated risk of neurological deficits. Moreover, because of the genetic basis, NF2-related tumors often recur, urgently necessitating the development of safe pharmacologic therapies for long-term tumor control in these patients.[3]

Biallelic inactivation of the *NF2* tumor suppressor gene is found in nearly all sporadic schwannomas regardless of their location.[4] Moreover, NF2 patients harbor germline heterozygous mutations in the *NF2* gene, and the related tumors exhibit additional loss or mutation of the remaining wild-type *NF2* allele. Thus, loss of function of the *NF2*-encoded protein, merlin/schwannomin, drives the initiation of essentially all schwannomas.[5]

Merlin is suggested to control cell proliferation by mediating contact inhibition of growth through mechanisms that include formation of stable adherens junctions and promoting efficient expression, activity, and transport of specific growth factor receptors.[6] Consequently, merlin loss activates numerous mitogenic pathways, including Ras/mitogen-activated protein kinase, Rac,

Received 23 September 2013; accepted 14 November 2013

phosphoinositide 3-kinase, and Hippo/Mst1, as well as E3 ubiquitin ligase activity in different cell types.[7]

Recently, merlin has been identified as a novel negative regulator of mammalian target of rapamycin complex 1 (mTORC1); functional loss of merlin was shown to result in elevated mTORC1 signaling in NF2-related tumors.[8] In addition, merlin-null mesotheliomas display deregulated mTORC1 signaling and are sensitive to rapamycin treatment.[9] Mammalian target of rapamycin is a ubiquitous protein kinase involved in several physiological processes, including cell survival, growth, proliferation, metabolism, and brain-specific functions, such as synaptic plasticity and cortical development.[10] Activation of the mTORC1 pathway has also emerged as a conserved regulatory mechanism in the control of cell size.[11]

Dysregulation of the mTOR pathway has been implicated in promoting a variety of pathological conditions, such as the tuberous sclerosis complex (TSC), perhaps the most studied example of a disease involving abnormal mTOR signaling. Mutation of either the *TSC1* or *TSC2* gene leads to abnormal activation of the mTOR pathway, resulting in increased cell growth and proliferation, promoting tumorigenesis in TSC patients.[12] Of direct translational relevance, clinical trials have shown that mTORC1 inhibitors can decrease growth of various tumors in TSC patients.[13] In fact, the mTORC1 inhibitor everolimus was recently approved by the FDA for the treatment of subependymal giant cell astrocytomas in TSC patients.[14]

Rapamycin (sirolimus) and rapalogs (the rapamycin analogs temsirolimus, everolimus, and deforolimus) are specific inhibitors of mTORC1. It remains unknown how rapamycin blocks mTORC1 activity, as it does not affect complex formation or autophosphorylation of mTORC1; however, it may affect the affinity of raptor interaction with the complex.[15] Recent reports suggest that prolonged treatment with rapamycin causes disintegration of mTORC1.[16] Although rapamycin inhibits primarily mTORC1 and not mTORC2, prolonged treatment of rapamycin can also inhibit mTORC2 by blocking its assembly and causing disintegration of mTORC2.[17,18] Unlike rapamycin and rapalogs, mTOR kinase inhibitors, the second generation of mTOR inhibitors is known as ATP competitive.[19] These mTORC1/mTORC2 dual inhibitors are designed to compete with ATP in the catalytic site of mTOR. Like rapalogs, they decrease protein translation, attenuate cell cycle progression, and inhibit angiogenesis in many cancer cell lines and in human cancer.

Similar to TSC proteins, merlin negatively regulates mTORC1 and positively regulates mTORC2. However, contrary to the activation of mTORC1 signaling, the attenuated mTORC2 signaling profiles in normal arachnoid and Schwann cells upon acute merlin loss are not consistently reflected in NF2-deficient meningiomas and schwannomas, suggesting that additional genetic events may be inconsistently acquired after initial merlin loss in these tumors.[20] Since mTORC1 activation underlies the aberrant growth and proliferation of NF2-associated tumors and may restrain the growth of these lesions through negative feedback mechanisms, we hypothesized that rapamycin, an inhibitor of mTORC1,[19] may be therapeutic for NF2.

Here, we show that rapamycin induced schwannoma growth delay in 3 complementary NF2 schwannoma mouse models. Moreover, in an NF2 patient with fast-growing VS, prolonged treatment with sirolimus inhibited tumor growth. Our findings provide evidence that mTOR inhibition should be explored in clinical trials for NF2-related schwannoma.

Materials and Methods

Cell Viability and Proliferation Assay

An ATP-based monolayer cell proliferation assay (Promega) and soft agar clonogenic assay were used to test cell viability and proliferation at 72 h and at 3 weeks, respectively, of drug administration in vitro. The drug concentration that inhibits cell growth by 50% (IC_{50}) was determined using GraphPad Prism 5.0 software. Details are in the Supplementary material.

Cell Size Analysis

Relative size of SC-FC912 cells (adult NF2-deficient mouse Schwann cells) with or without rapamycin treatment was obtained by fluorescence-activated cell sorter (FACS) analysis (FACSAria, Becton Dickinson) using forward scatter-height (FSC-H). Cells were treated with 20 nM or 20 μM of rapamycin every day for 4 days. Cells were trypsinized, fixed with ethyl alcohol 70%, and incubated with RNase (100 μg/mL) and propidium iodide (5 μg/mL). A total of 20 000 cells were collected, and the mean FSC-H value of the G1-phase cell population was obtained from FACSDiva software as a measure of relative cell size (6000–12 000 cells). A cell count graph was realized with FlowJo software.

Cell Surface Area Measurements

Human schwannoma cell primary cultures were freshly prepared from surgical samples. After incubation for 1–5 days in Proliferation Medium (PM) (Dulbecco's modified Eagle's medium with 10% fetal calf serum [Invitrogen], 1% N2 supplement, 10 ng/mL neuregulin-1 and 2 μM forskolin, 50 μg/mL gentamycin, and 1% Fungizone), tissues were dissociated for 4 h or overnight with 0.05% collagenase type I (Invitrogen) and 1.25 U/mL dispase (Roche). Cells were plated in 12- or 24-well plates coated with poly-L-lysine (Sigma)/laminin (Invitrogen) and cultured at 37°C in 7.5% CO_2. Cells were plated at 1000 or 2000 per well and used between passages 2 and 4. Rapamycin was added at the different concentrations 4–5 days after plating, and medium was then changed with new drug every other day for 12–20 days. Cells were fixed in 4% paraformaldehyde and stained with anti-S100 protein (Dako Z0311), followed by Al594-conjugated goat anti-rabbit secondary antibody (Life Technologies) and counterstained with Hoechst 33258 (Life Technologies). Cell surface areas were determined using the automated Celigo Cell Cytometer (Brooks Life Science Systems). An average of 450 (min 328, max 580) or 900 (min 655, max 1130) cells were quantified per well of 12- or 24-well plates, respectively.

Western Blot and ELISA

Tumor specimens of vehicle- or rapamycin-treated mice were snap-frozen in liquid nitrogen and stored at −80°C. Pulverized frozen tumor samples were lysed in radioimmunoprecipitation assay (RIPA) buffer and the total proteins were extracted, separated, and transferred using standard procedures. Antibodies used for western blotting are in Supplementary material. Levels of S6, phospho-S6 (Ser235/236), Akt, phospho-Akt1 (Ser473), phospho-4E-BP1 (Thr37/Thr46), and alpha-tubulin were determined using the PathScan Cell Growth Multi-Target Sandwich ELISA Kit (Cell Signaling Technology) following the manufacturer's recommendation.

Allograft Models and Antitumor Efficacy Assay

All animal care and experimentation reported herein were performed in strict adherence to the National Institutes of Health (NIH) guidelines in the US Public Health Service Policy on Humane Care and Use of Laboratory Animals and with the specific approval of the Institutional Animal Care and Use Committee (IACUC) under protocol number HE1175-08-03. The SC4-9

cells and the transplantable schwannoma homogenate, 08031-9, were grafted in *nu/nu* and in Friend virus B (FVB)/N syngeneic mice, respectively. Details and morphometric analysis of intratumoral vasculature are in Supporting Information.

Compound and Administration

Aliquots containing 20 mg/mL rapamycin diluted in ethanol were prepared weekly and stored at −20°C. Each aliquot was then diluted in vehicle (0.25% polyethylene glycol 400, 0.25% Tween 80, H_2O) <1 h before use, to obtain a final dosing of 10 mg/kg/day. Rapamycin treatment was dosed 8 mg/kg/day and administered by intraperitoneal injection following a schedule of once a day, 5 of 7 days for the ESC-FC1801 xenografts (14 d treatment), 08031-9 syngrafts (36 d treatment followed by 14 d withdrawal for 3 mice), and P0-SCH-Δ(39-121)-27 transgenic mice during the first 2 months of treatment. In the latter model, following this initial regimen, rapamycin was then dosed 16 mg/kg weekly during 8.5 months, followed by the original regimen for the last 1.5 months (1 y of treatment). A regimen including daily administration 7 of 7 days was used for the SC4-9 intraneural orthotopic xenograft experiment (15 d of treatment). For SC4-9 grafts, tumor volumes were calipered and body weight was measured during the course of the experiment. Treatment was stopped at day 36 because the mean tumor volume of the control group reached the IACUC approved volume. At that time, tumors were dissected for pharmacokinetic-pharmacodynamic analysis.

Pharmacokinetic Analysis

The concentration of rapamycin in plasma and tumors was measured following single dose and repeated dose administration. The assay was performed by Rocky Mountain Instrumental Laboratories. Details are in the Supplementary material.

Morphometric Analysis of Schwann Cell Tumorlets in NF2 Transgenic Mice

P0-SCH-Δ(39–121)-27 transgenic mice in the FVB/N background[21] were bred to wild-type C3H mice to generate (FVB/NCrlxC3H/HeNCrl)F1. Mice were randomized to receive rapamycin or vehicle at 6 weeks of age, corresponding to the time of tumor induction in this model. The development of Schwann cell tumorlets in the spinal nerve roots was histopathologically scored at the endpoint and compared between drug-treated and vehicle-treated mice. Details are in Supporting Information.

Immunohistochemical Analysis

Three-micrometer-thick formalin-fixed, paraffin-embedded sections were immunostained following manufacturers' recommendations and standard protocols with antibodies against the following antigens: phospho-S6 (1:1000 or 1:200; #2211, Cell Signaling Technology), phospho-Akt (1:100; #4060, Cell Signaling Technology), CD31 (1:750; sc-1506, Santa Cruz Biotechnology), hypoxia-inducible factor–1α (sc-10790, Santa Cruz Biotechnology), and LC3 (NBP1-19167, Novus Biologicals). To assess cell proliferation, we used bromodeoxyuridine (BrdU; Invitrogen) labeling of cells in S phase of the cell cycle. Bromodeoxyuridine (50 μg/g body weight) was administrated 4 h before harvesting tissues for xenograft experiments or 3 times at 3-h intervals (24, 21, and 18 h) before dissection for the P0-SCH-Δ(39-121)-27 transgenic mice. Incorporation of BrdU was then revealed following manufacturer recommendations (BrdU Staining Kit, Invitrogen). Apoptosis was monitored on formalin-fixed paraffin-embedded sections using the DeadEnd Colorimetric TUNEL System (Promega) following manufacturer recommendations.

Data Analysis

For measurements, data are expressed as mean ± SEM. For statistical comparison at the endpoint, we used either a Student's *t*-test or Mann–Whitney test when appropriate (2-tailed for unequal variance). For longitudinal follow-up of tumor growth in the subcutaneous graft models or mice weight, we used a nonparametric Wilcoxon test (2-tailed for unequal variance). For all tests, the level of significance was set at $P < .05$ (2-tailed), P values: *<.05, **<.01, ***<.001. Statistical calculations were done using GraphPad Prism 5.0a. For comparison of tumor response in the P0-SCH-Δ(39-121) transgenic mice and to handle dependencies between observations we used a multilevel analysis (SPSS 18.0). A Kaplan–Meier curve and a log-rank test were used to compare the delay before occurrence of a severe paralysis in the intraneural orthotopic model (GraphPad Prism 5.0a).

Human Subjects

Informed consent was obtained from the subject, and the experiments conformed to the principles set out in the World Medical Association's Declaration of Helsinki (http://www.wma.net/en/30publications/10policies/b3/) and the NIH Belmont Report (http://ohsr.od.nih.gov/guidelines/belmont.html).

Volumetric Tumor Monitoring

Tumor volumes were calculated on 3D T1 gadolinium-enhanced MRI sequences (slice thickness, 1 mm, no skip) by manual segmentation with OsiriX 4.0 software (Pixmeo). Using ITK SNAP 2.4.0 software, the volume of the cystic components was calculated on 3D T1 gadolinium-enhanced sequences by user-guided 3D active contour segmentation.[22]

Results

Merlin-deficient Schwannoma Cell Lines Are Sensitive to Rapamycin

NF2 inactivation results in the aberrant activation of the mTOR pathway, raising the possibility that growth and survival of NF2-associated tumors may be dependent on increased mTOR signaling.[8,9,23,24] To test this hypothesis, we first examined the effects of rapamycin on human and murine merlin-deficient schwannoma cell lines. The proliferation of mouse schwannoma cells (08031-9) was potently inhibited by low doses of rapamycin, with IC_{50} values <0.1 nM. Long-term effect of rapamycin in merlin-deficient cells in vitro was evaluated by soft agar clonogenic assay. Because of their benign nature, primary cultures of schwannoma cells do not form colonies in this assay and were therefore excluded from the analysis. Soft agar clonogenic assays using 3 immortalized cell lines—*Nf2*$^{-/-}$ mouse Schwann cells (ESC-FC1801) and mouse (08031-9) and human (HEI193) schwannoma cells—showed significant reduction in the number of anchorage-independent colonies, in a dose-dependent manner, in all cell lines (Fig. 1A and B). Significant reduction was evidenced at 1 nM rapamycin exposure for 21 days, compared with the vehicle-treated control ($P <$ .001). There was no statistical difference between the 1 and 100 nmol/L rapamycin doses in terms of colony numbers. As predicted from previous studies showing that rapalogs are cytostatic, not cytotoxic, colony growth resumed upon rapamycin withdrawal, and the number of colonies was not significantly different from that in the vehicle-treated control after an additional 21 days of withdrawal (Fig. 1A and B). Consistent with these results, we also

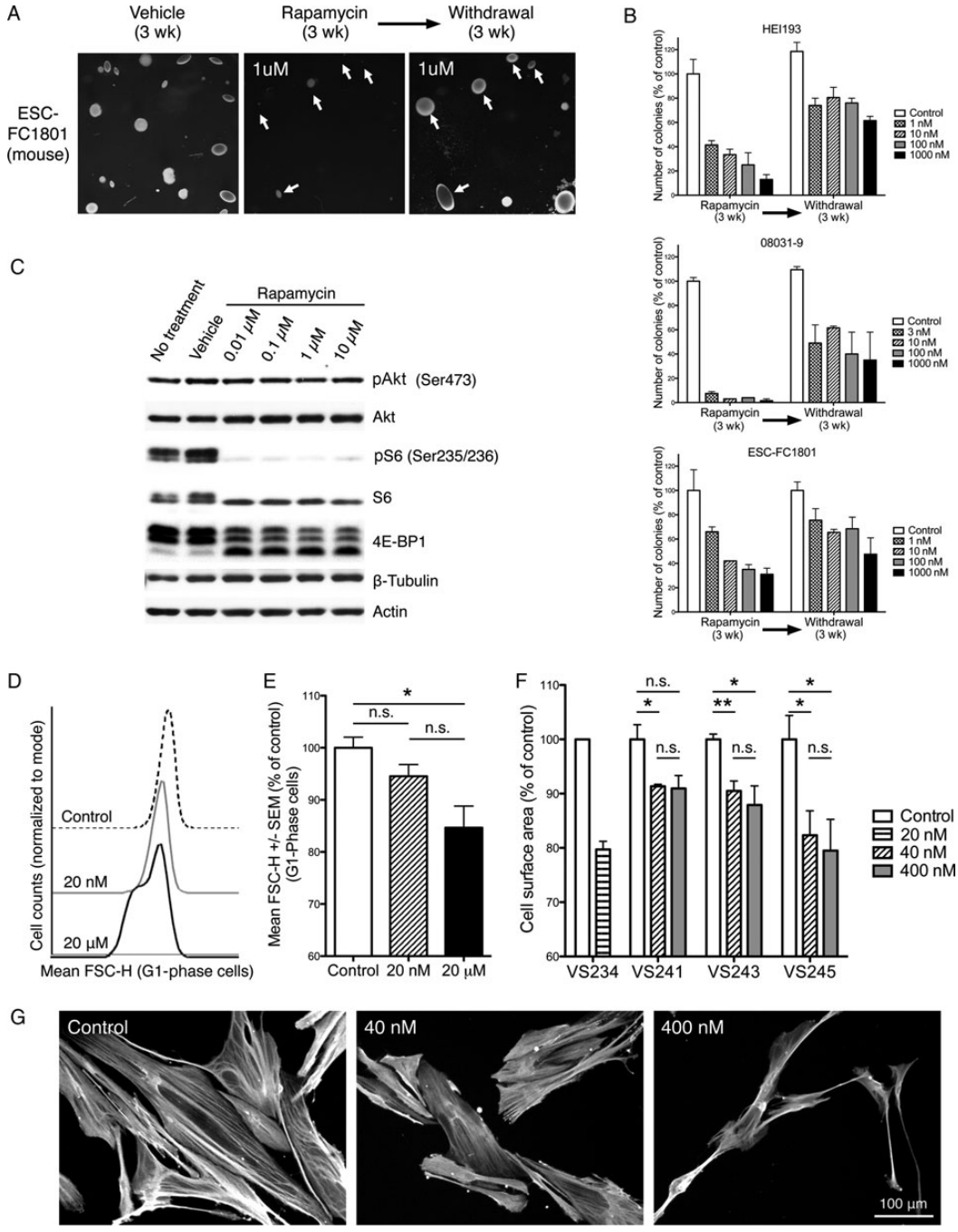

Fig. 1. Rapamycin inhibits growth and reduces cell size of human and murine *NF2*$^{-/-}$ schwannoma cells. (A and B) Soft agar colony formation assay was performed with the HEI193 human schwannoma cell line, the 08031-9 mouse schwannoma cell line, and ESC-FC1801 mouse *Nf2*$^{-/-}$ Schwann cells. After 3 weeks of treatment, the number of colonies was evaluated for the different concentrations of rapamycin or vehicle treatment, and reduction in colony formation was shown with rapamycin treatment. Then, the same plates were incubated without rapamycin for an additional 3 weeks: the increased number of colonies demonstrated a cytostatic effect of rapamycin. (C) The 08031-9 mouse schwannoma cell line was treated with different concentrations of rapamycin or with vehicle or not treated for 24 h. Western blot analysis showed strong inhibition of S6 and 4E-BP1 phosphorylation without increase of Akt phosphorylation. p-Akt, phosphorylated Akt. (D and E) Mouse *Nf2*$^{-/-}$ Schwann cells were treated with rapamycin at 20 nM and 20 μM, harvested, stained with propidium iodide, and analyzed by flow cytometry to determine FSC-H of G1-phase cells. (D) Shift of FSC-H with rapamycin treatment for one experiment. (E) FSC-H average for 3 independent experiments. (F and G) Primary cultures of human schwannoma cells were treated with rapamycin at 20 nM, 40 nM, or 400 nM for 12–20 days then fixed and stained for S100 protein (G). The cell surface area of S100 protein–positive cells was assessed with an automated Celigo Cell Cytometer. The 4 VS cell cultures showed a reduction of the mean cell area after rapamycin treatment (F). Data on VS234 were not the result of performance in triplicate, therefore statistical significance is not provided. Error bar of VS234 cells treated with 20 nM are relative to duplicate wells.

found that rapamycin functions by triggering growth arrest of schwannoma cells rather than apoptosis measured in vitro using a caspase activity assay (not shown). To clarify the underlying mechanisms that control this antiproliferative effect, we treated 08031-9 cells with rapamycin for 24 h and then monitored phosphorylation of S6 and 4E-BP1 in cell lysates by western blot (Fig. 1C). As expected, rapamycin blocked the phosphorylation of S6 and decreased the phosphorylation of 4E-BP1, whereas vehicle had no effect. As Akt phosphorylation can be secondarily upregulated following mTOR inhibition, we tested whether the phosphorylation of Akt was altered in response to rapamycin. No increase in phospho-Akt was observed in 08031-9 cells treated with rapamycin, at least at this start time.

Primary cells of human merlin-deficient schwannoma and meningioma exhibit an enlarged-cell phenotype compared with nonneoplastic cell counterparts,[8,23,24] and exposure to rapamycin has been shown to revert them to this phenotype in meningioma cells.[8] An analysis of relative cell sizes by flow cytometry demonstrated that *Nf2*$^{-/-}$ mouse Schwann cells that were actively dividing and had been treated with rapamycin for 4 days were strikingly smaller in size compared with nontreated cells, as indicated by a decreased FSC-H mean (Fig. 1D and E). Similarly, primary cells from human vestibular schwannomas treated with rapamycin for 12–20 days demonstrated a reduced cell surface area compared with nontreated cells (Fig. 1F and G). These findings indicate that as in meningioma cells, inhibition of mTORC1 by rapamycin also reduces the size of merlin-deficient schwannoma cells.

In vivo Response to Rapamycin Treatment in Mice

To test the requirement for mTOR in NF2 tumorigenesis in vivo and to assess the preclinical therapeutic efficacy of rapamycin, we used 3 mouse models of *Nf2*-mutant schwannoma.

First, we used 2 allograft models as relatively high throughput preclinical evaluation systems relevant to NF2-related schwannomas. In one model, orthotopic grafts were generated by injecting *Nf2*$^{-/-}$ mouse Schwann cells, SC4-9, into the sciatic nerves of *nu/nu* mice. The other is a syngeneic, transplantable subcutaneous allograft model derived from a schwannoma (08031-9) that arose spontaneously in a transgenic P0-SCH-Δ(39-121)-27 mouse.

For the third model, we used a genetically engineered mouse NF2 model: the transgenic P0-SCH-Δ(39-121)-27 mice, which express a dominant-negative human merlin mutant protein in Schwann cells, resulting in functional inactivation of endogenous merlin. This model features schwannosis (Schwann cell hyperplasia and tumorlets) and frank schwannomas that develop primarily within the spinal roots and other peripheral nerves.[21,25,26] The rapid development of endogenous lesions and their predictable progression represent a powerful model for preclinical drug testing for NF2.

Daily administration of rapamycin at 8 mg/kg/day was well tolerated with no significant weight loss in any animals tested in this study (not shown). Since the standard rapamycin dosing regimen in humans is 3–20 ng/mL, the dose used in our study was relevant to rapamycin treatment in humans.[27] In the 2 allograft NF2 models (Figs. 2A and 3A), rapamycin potently suppressed merlin-deficient tumor growth (Fig. 2B and C and Fig. 3C and D), with a significant cytostatic effect demonstrated by a reduced number of BrdU-positive cells (Figs. 2E and 3G) and no change in apoptosis (not shown). In addition, rapamycin exposure delayed onset and reduced the penetrance of severe hind-limb paralysis, an additional functional preclinical endpoint in the sciatic allograft model (Fig. 2D). The concentration of rapamycin in the 08031-9 tumors after repeated administration reached above 200 ng/mg, a dose equivalent to ~220 nM in vitro (Fig. 3B).

Inhibition of S6 and 4E-BP1 phosphorylation was observed in treated tumors, demonstrating that rapamycin effectively suppressed the mTOR pathway in vivo (Fig. 2G and H and Fig. 3E and H). Tumor growth inhibition was dependent on continuous exposure to rapamycin, as after rapamycin withdrawal tumors reexhibited S6 phosphorylation and resumed growth at a faster rate than vehicle-treated tumors (Fig. 3C, E, H). As Akt phosphorylation can be upregulated following mTOR inhibition,[28] we tested whether the phosphorylation of Akt was altered in response to rapamycin. A small increase in phospho-Akt was observed in tumor samples treated with rapamycin compared with vehicle-treated tumors (Figs. 2I and 3I). Taken together, these data demonstrate that merlin-deficient tumors can be almost completely contained by a continuous treatment with an mTOR inhibitor. The enhanced in vivo effect of rapamycin correlated with decreased vascularization of the tumors (Fig. 2F and Fig. 3F and J), suggesting that rapamycin effects may be at least in part mediated via effects on the vasculature. The rebound effect of rapamycin in the mouse schwannoma is similar to the transient response to RAD001 observed in malignant peripheral nerve sheath tumor, hemangiosarcoma, or glioblastoma xenograft models.[29,30]

Next, we utilized the genetically engineered mouse model of NF2-related schwannoma. P0-SCH-Δ(39-121)-27 transgenic mice in the (FVB/NCrlxC3H/HeNCrl)F1 background were randomized to receive either rapamycin (8 mg/kg/d) or vehicle, 5 days per week. Treatment was started when mice were 6 weeks old and continued for 8 weeks (Fig. 4A). The efficacy of rapamycin treatment in this model was assessed by comparing the tumor burden, as defined by the ratio of tumoral versus normal nerve in the spinal roots (Fig. 4B). The mean percentage of tumor area/total root area in the rapamycin-treated group was 4.4% and in the vehicle-treated group 16.8% (Fig. 4E). This 75% decrease of the tumor load was statistically highly significant ($P < .001$, multilevel analysis; SPSS). To monitor the effect of rapamycin on the mTOR targets S6K and 4E-BP1 in this model, we treated 4 mice with rapamycin and 4 mice with vehicle during 7 days. The spinal nerves containing the tumors were dissected and analyzed by western blot (Fig. 4C), which showed a strong reduction of S6 and 4E-BP1 phosphorylation. We also observed a slight increase of Akt phosphorylation in treated mice (Fig. 4C). Finally, we examined the efficacy of a prolonged maintenance dose of rapamycin over a course of 12 months using a similar schedule previously reported in a mouse model of tuberous sclerosis.[27] Nine mice at 6 weeks of age were assigned to rapamycin treatment, while 7 mice received vehicle as control. After 2 months of daily administration of rapamycin (8 mg/kg/d, 5 d/wk), treatment was continued weekly for 9 months (16 mg/kg/d, 1 d/wk), and then daily for 1.5 months (8 mg/kg/d, 5 d/wk) (Fig. 4A). We observed a 40% reduction in Schwann cell tumors in drug-treated mice (Fig. 4E). Remarkably, rapamycin treatment delayed tumor growth by 7 months over the course of the 12-month treatment (Fig. 4D), and treatment was well tolerated. However, 3 female mice in the rapamycin-treated arm were euthanized because of uterus tumors, previously

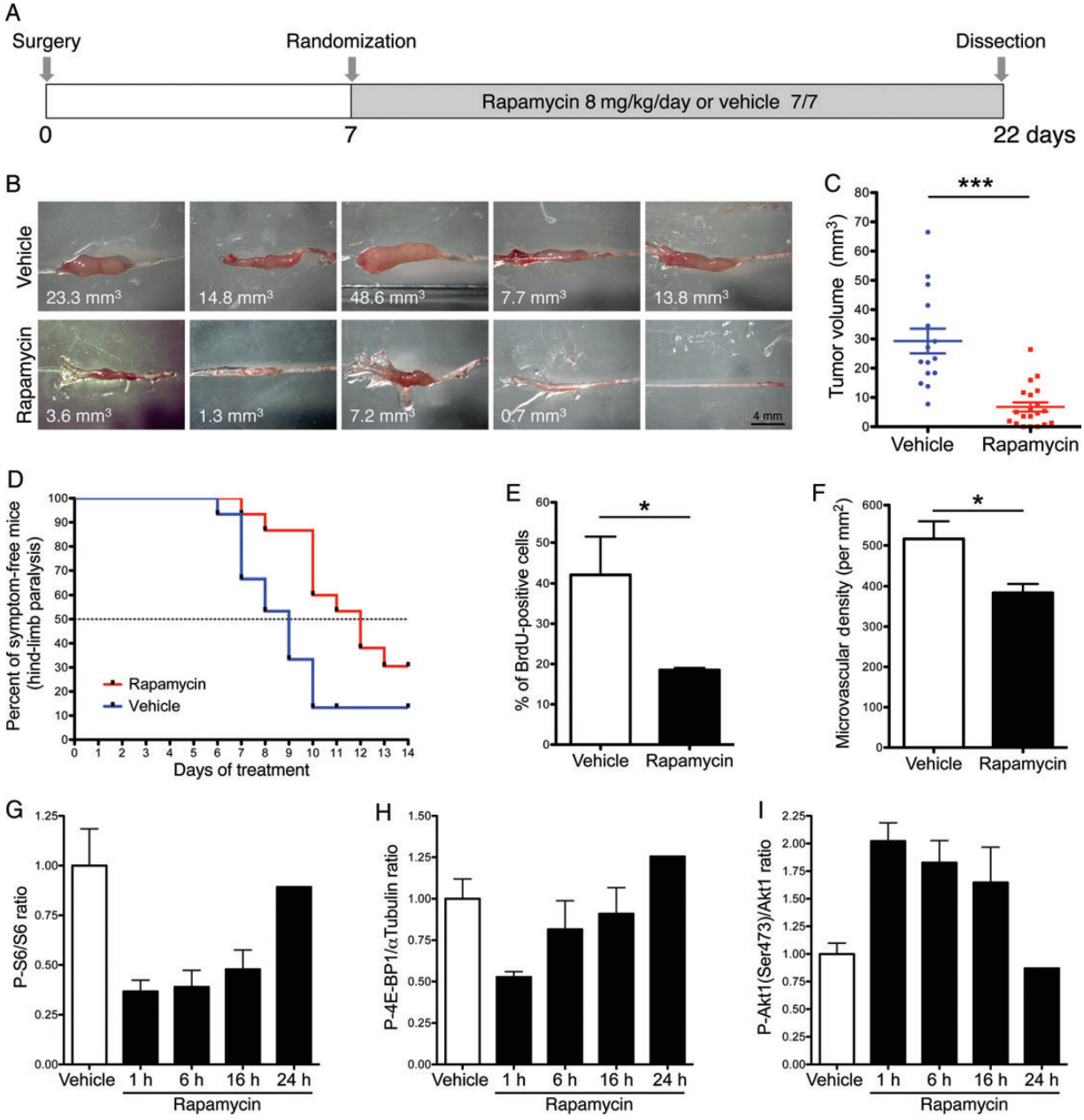

Fig. 2. Rapamycin rapidly inhibited tumor growth and improved functional outcomes in an orthotopic NF2 mouse schwannoma allograft model. (A) *Nu/nu* mice were implanted with adult mouse *Nf2*$^{-/-}$ Schwann cells 1 week before randomization. Mice were treated daily with rapamycin (8 mg/kg/d, i.p.) ($n = 20$) or vehicle ($n = 15$) for 14 days. (B and C) Rapamycin treatment reduced the growth of intraneural *Nf2*$^{-/-}$ Schwann cell allografts by 4-fold compared with vehicle-treated controls ($P = .001$ at day 22) and (D) significantly delayed the onset of severe hind-limb paralysis. (E and F) Rapamycin treatment reduced the number of BrdU-positive cells (E) and microvascular density (F) in tumors. (G–I) Quantification of absorbance for phospho-S6 protein normalized to total S6 by ELISA demonstrated decreased phosphorylation at 1 h, 6 h, and 16 h following i.p. administration of 8 mg/kg/d rapamycin (G). Maximum inhibition was observed at the 1-h time point. Phospho–4E-BP1 levels normalized to α-tubulin were also decreased, confirming inhibition of the mTOR pathway 1 h after drug administration (H). However, likely due to the existence of a negative feedback loop emanating from S6K,[28,47] we noted that rapamycin transiently activated Akt (I).

reported in this model.[21] Based on the natural history of Schwann cell tumor growth in this model (blue curve in Fig. 4D), we defined histopathological progression as a tumor area/total nerve area of 25%, resulting in 7 months of time to tumor progression in untreated mice. Based on this definition, a 2-fold increase of time to tumor progression was achieved in the rapamycin arm.

Sirolimus Induces Vestibular Schwannoma Growth Arrest in an NF2 Patient

Concomitant with these preclinical studies, a 29-year-old NF2 patient with uncontrolled fast-growing peripheral schwannomas was offered an experimental course of sirolimus therapy. This

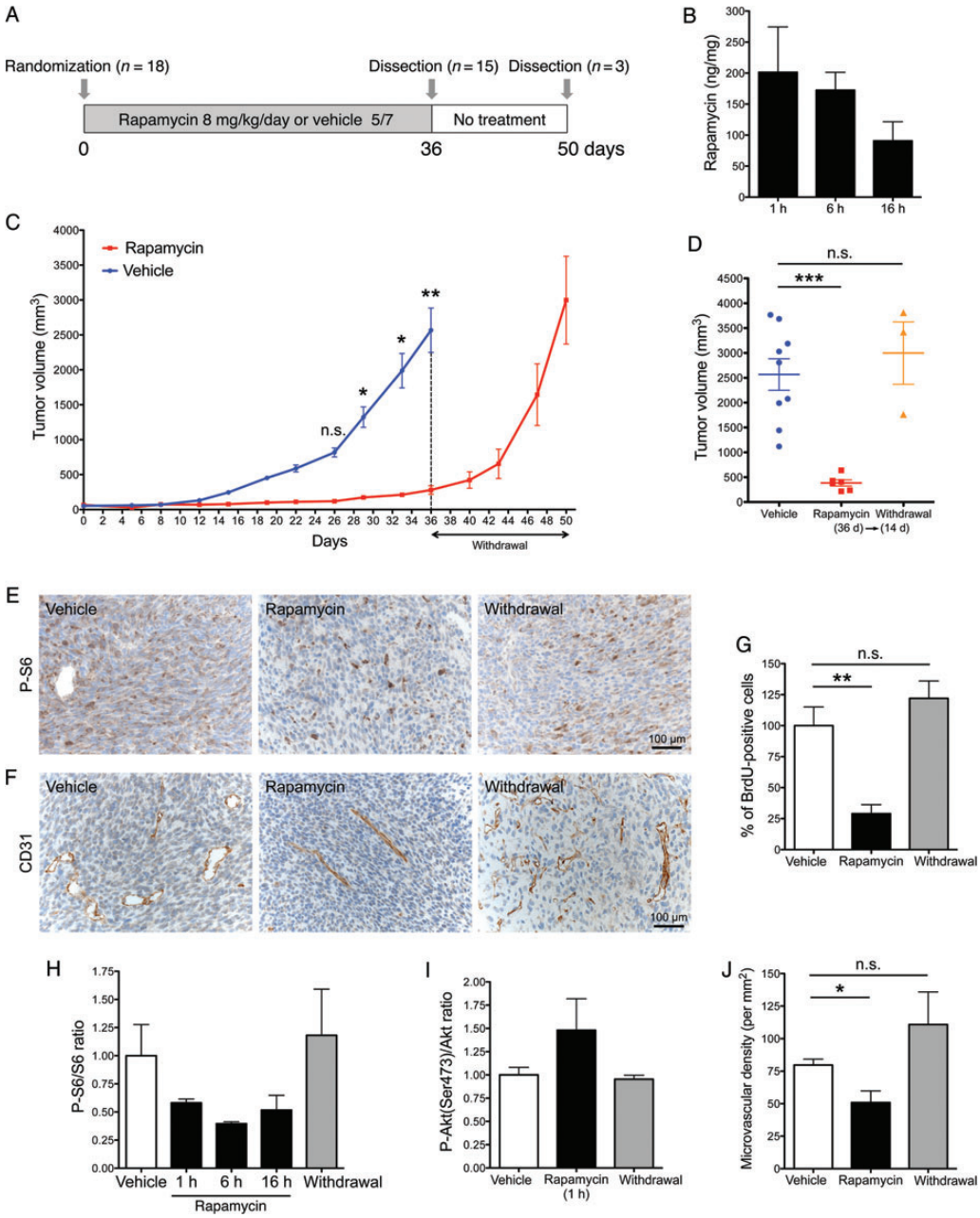

Fig. 3. Rapamycin suppresses the growth of a transplantable mouse schwannoma model. (A) Mice bearing 08031-9 tumors were treated with rapamycin 8 mg/kg/d for 5/7 days per week for 36 days. For 3 mice, treatment was discontinued for 14 days before sacrifice. (B) Pharmacokinetic analysis of rapamycin-treated mice showed that rapamycin concentration levels in tumors reached levels consistent with activity in vitro. (C) Rapamycin potently suppressed schwannoma growth, showing potent cytostatic effects ($P = .0004$ at the endpoint, Mann–Whitney test). Three mice in the treated group were kept without treatment to evaluate the effect of rapamycin withdrawal on tumor growth, showing that rapamycin-induced inhibition of tumor cell proliferation was reversible. (D) After 36 days of treatment, the rapamycin-treated group demonstrated reduction in tumor volume >5-fold compared with controls ($P < .001$, *t*-test). (E–J) Rapamycin treatment inhibited mTOR activity and activated Akt. (E) Phospho-S6 protein immunohistochemistry in vehicle- and rapamycin-treated tumors showed decreased phosphorylation at 1 h after rapamycin administration. (F) CD31 immunohistochemistry highlights abnormal vascular morphology and increased vessel diameter in the vehicle and withdrawal groups. Tumor vessel morphology was improved in the rapamycin-treated group. (G) Quantification of BrdU incorporation demonstrated significant reduction of proliferating tumor cells following rapamycin treatment ($P = .0018$ vs vehicle). Fourteen days after treatment withdrawal, the proliferating index regained the control level. (H) Quantification of absorbance for phospho-S6 protein normalized to total S6 by ELISA showed decreased phosphorylation at 1 h, 6 h, and 16 h. Maximum inhibition was observed at the 6-h time point. (I) As a result of mTOR inhibition, densitometry-quantified levels of phospho-Akt normalized to total Akt showed activation 1 h after the last rapamycin dose. (J) Quantification of intratumoral vascular density (iMVD) evaluated in vehicle ($n = 6$), rapamycin ($n = 4$), and withdrawal ($n = 3$) groups demonstrated a significantly decreased iMVD in the treated group ($P = .012$ vs vehicle). Increased iMVD was observed after drug withdrawal ($P =$ ns vs vehicle).

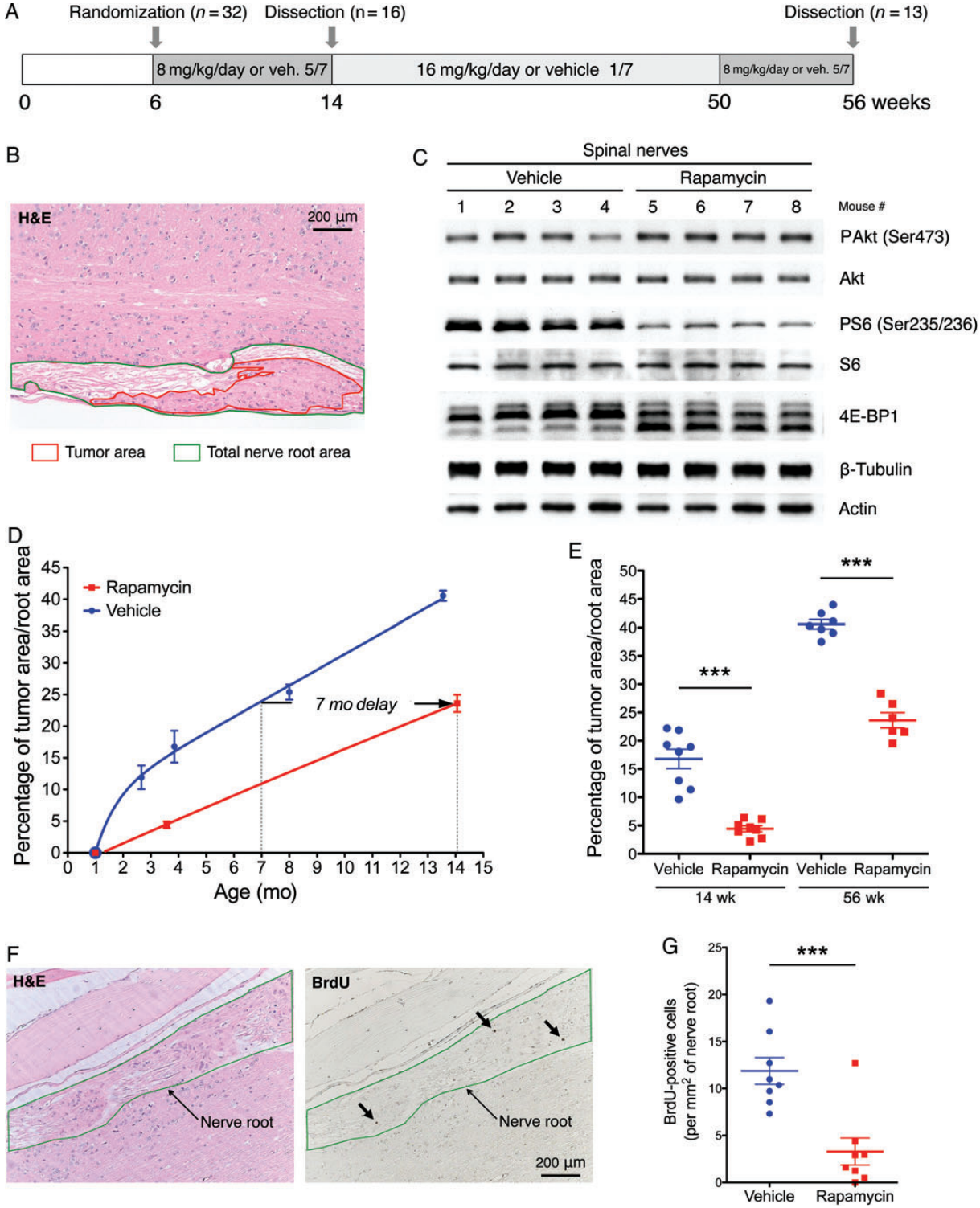

Fig. 4. Rapamycin inhibits tumor growth in an NF2 schwannoma genetically engineered mouse model. (A) Starting at 6 weeks of age, transgenic P0-SCH-Δ(39-121)-27 mice were randomized and treated daily with rapamycin (8 mg/kg/d, i.p., 5/7 d/wk) ($n = 14$) or vehicle ($n = 15$) for 8 weeks. After 8 weeks of treatment, 8 mice/group were analyzed, while the remaining mice ($n = 13$) were treated following a weekly regimen of rapamycin (16 mg/kg/d, i.p., 1/7 d/wk) or vehicle until 50 weeks old, when the initial drug regimen was resumed for 6 additional weeks. (B) For each mouse, the surface ratio between tumoral and normal nerve tissue was calculated. H&E, hematoxylin and eosin. (C) Transgenic P0-SCH-Δ(39-121)-27 mice were treated during 7 days with rapamycin (8 mg/kg/d) or vehicle. Spinal nerves were collected 1 h after the last dose, and protein was analyzed by western blot, showing decreased phosphorylation of S6 and 4E-BP1 proteins and a slight increase in Akt phosphorylation. (D) Natural history of Schwann cell tumor

patient had had a diagnosis of NF2 at age 10 due to unilateral hearing loss. MRI revealed bilateral VSs, several cranial meningiomas, lower cranial nerve schwannomas, and spinal tumors including ependymomas. He harbored a stop mutation in exon 4 of *NF2* on blood test (c.373C > T) and was the only affected member of his family. As a result of spinal tumors, brachial plexus schwannomas, and peripheral neuropathy, he had a complete paralysis and amyotrophy of his left upper limb. At age 15, he became deaf on the right side, and his 15-mm right VS was irradiated by gamma knife. He became deaf on the left side at age 19, and the left VS was removed at age 24 because of progressive enlargement. Insertion of an auditory brainstem implant failed because of cerebellum edema. He developed efficient lip reading and lived an independent life, working as a pharmacist. Despite gamma knife treatment, the left VS grew regularly at a mean rate of 47% per year in volume between ages 26 and 30, reaching 24.9 cm^3. At age 29, right-hand paresis progressively occurred, associated with an increase in size of a huge tumor invading all the branches of the brachial plexus. Surgical removal of this tumor was not possible.

Thus, in 2009, at age 30, sirolimus (Rapamune, Pfizer) was introduced on a compassionate use basis. Oral doses were gradually increased from 0.4 mg to 6 mg a day, and sirolimus trough levels steadily reached 17 ng/mL (Fig. 5A). Follow-up included clinical examination, blood tests, and MRI. The patient has now been under sirolimus for 4.5 years, without noticeable secondary event (grade 1 diarrhea according to the Common Terminology Criteria for Adverse Events v3.0). A decrease in VS growth rate was obvious (Fig. 5A and B), from 47% per year (from 9.1 to 24.9 cm^3 in 3.7 y) before treatment to 5.2% per year (from 24.9 to 27.7 cm^3 in 2.1 y). We even observed a decrease in VS volume from 28.8 to 27.7 cm^3 (−3.8%), during a 5-month period (−8.8%/y), corresponding to the highest dose period (5 to 6 mg/d, blood levels 16–27 ng/mL). Of note, other cranial schwannomas and meningiomas remained stable during follow-up, except 1 meningioma (grade II) on the anterior skull base that enlarged with progressive vision loss and was removed at age 32. Sirolimus was discontinued for a 2.5-month period encompassing the surgical procedure. We observed an increase in VS growth rate, which reached 22% per year during this period (from 27.7 to 29.7 cm^3 in a 4-mo interval between MRIs). Reintroduction of sirolimus at 4 mg a day (plasma levels 16–17 ng/mL) led to a new decrease in VS growth rate to 3.5% per year (from 29.7 to 31.9 cm^3 in 2 y) (Fig. 5A). A 20% variation in tumor volume is usually used as an endpoint in NF2 trials.[35] In this patient, the times needed for a 20% increase of tumor volume were 9 months before sirolimus treatment and 30.5 months after sirolimus onset. Thus, we observed a 3.4-fold increase in time to tumor progression under sirolimus therapy. Of note, the brachial plexus schwannoma remained stable, although precise volume evaluation was not performed because of the involvement of several branches of the brachial plexus. Clinically, a stabilization of the right-hand paresis was noticed. We also noticed cystic changes of VS during sirolimus treatment: at treatment onset, scarce patchy cystic areas were visible on MRI. The cystic component of VS reached 10.3% of tumor volume at last follow-up (Fig. 5B). These cystic modifications or loss of contrast enhancement are observed frequently after radiosurgery and are considered a good prognostic indicator of tumor regression.[31] These changes could also reflect the response to sirolimus, similarly to what is described in response to targeted therapies that do not induce frank tumor shrinkage, despite improved patient outcome.[32] Although reflecting the course of a single patient, this clinical outcome is remarkably consistent with the preclinical studies in NF2 mice described above. Altogether, our results indicate that prolonged treatment with low doses of mTORC1 pathway inhibitors may result in long-term stabilization of growing NF2-related schwannomas and strongly support the evaluation of this strategy in clinical trials.

Discussion

NF2 is a rare autosomal dominant genetic disorder caused by inactivation of the tumor suppressor gene *NF2*.[33] Interestingly, though NF2 affects only 1:33 000 persons with a prevalence of 5466 affected people alive in the United States,[34] population studies suggest that up to 1:300 people will develop a tumor with an underlying sporadic *NF2* mutation in their lifetime.[35] NF2 represents a difficult management problem, with most patients facing substantial morbidity and reduced life expectancy.[36] Until recently there were few pharmacologic options for individuals with NF2. With increasing understanding of the genetic basis of the disease, as well as emerging molecular parallels with various cancers for which drug therapies are in development or already clinically available, therapeutic development for NF2 is also progressing. Nevertheless, challenges lie ahead for NF2, including the definition of functional endpoints for clinical evaluation strategies.

Time to tumor progression as an endpoint has not yet been used for NF2 VS studies, although in the case of these slow-growing, indolent tumors, delaying progression would be a highly desirable outcome, especially if accompanied by acceptable hearing and neurologic performance with good quality of life. Our preclinical study in a genetically engineered mouse NF2 model, which recapitulates schwannoma natural history, demonstrated that rapamycin significantly increased time to tumor progression and was well tolerated over an extended period of time. In addition, grafted tumor regrowth was observed upon cessation of therapy, consistent with the known cytostatic rather than cytotoxic effects of rapamycin. Our findings show that rapamycin alone limits but does not suppress tumorigenesis, as observed in mouse models of tuberous sclerosis. Blocking mTORC1 signaling with rapamycin also results in elevated phospho-Akt.[28] As Akt is a progrowth, prosurvival molecule, this feedback loop must be considered when treating NF2 tumors with rapamycin. Whether rapamycin treatment would be effective only in NF2 tumors or equally effective in sporadic schwannomas and meningiomas with *NF2* mutations is not

development in the transgenic P0-SCH-Δ(39-121)-27 mice. The maintenance regimen delayed the growth of spinal root tumors compared with the predicted tumor burden in untreated mice. (E) Average tumor burden ± SEM in the spinal roots (40 ± 4 per mouse) is presented as a tumor ratio at the end of 14 weeks and 56 weeks of treatment ($P < .001$, multilevel analysis). (F) BrdU injections were performed in rapamycin- and vehicle-treated mice. The green line shows the nerve root area where the BrdU-positive cells were counted. H&E, hematoxylin and eosin. (G) Quantification of BrdU-positive cells showing reduction of proliferation in rapamycin-treated mice (56 wk treatment).

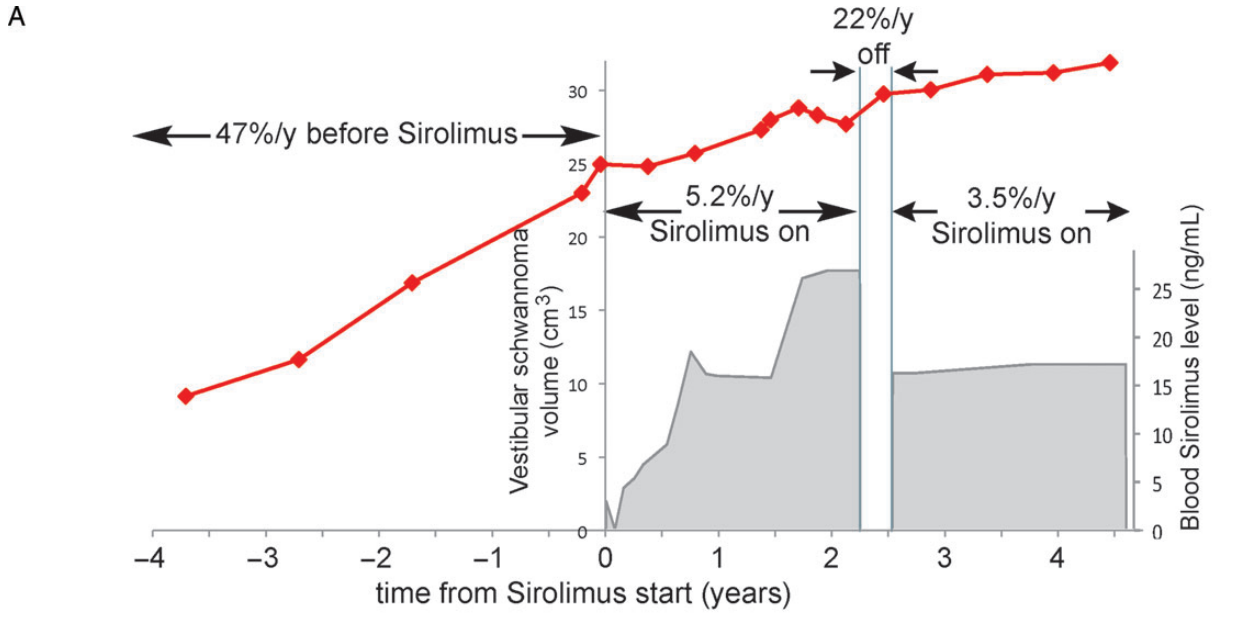

Volumes (cm3)				
VS	9.1	24.9	27.7	31.9
cysts	0.0023	0.31	2.0	3.3
% cysts	0.025	1.2	7.2	10.3

Fig. 5. Volumetric evolution of VS in an NF2 patient treated with sirolimus. (A) Annual volumetric tumor growth of the right VS decreased under sirolimus therapy from 47% per year to 3.5% per year. Sirolimus blood dosages are indicated in the lower right part of the graph. (B) T1 axial gadolinium-enhanced sequences showing the target VS at 4 different time points during evolution (identical scale bar in each MRI = 1 cm). The table shows the volume of VS and the corresponding cystic component during sirolimus therapy.

known. Recently, mTORC1 inhibition has been shown to suppress meningioma growth in mouse xenograft models, and increased Akt phosphorylation was observed in the treatment group.[37] Since Akt activation in meningiomas has been associated with higher grades, the feedback activation of Akt upon mTORC1 inhibition should be particularly considered when treating these tumors.[38]

The in vivo effect of rapamycin correlated with decreased perfusion of the tumors, suggesting that rapamycin effects may be at least in part mediated via effects on the vasculature. In NF2 patients, hearing decline is significantly more common with actively growing tumors,[39] thus stabilization of tumor growth could also result in hearing preservation. The mTOR pathway has been implicated in the regulation of tumor production of proangiogenic factors as well as modulation of vascular endothelial growth factor receptor signaling in endothelial cells. Encouraging results have been reported with bevacizumab (Avastin, Genentech), a humanized monoclonal antibody directed against vascular endothelial growth factor, in treating NF2 patients on a compassionate use basis. About 40% of NF2 patients achieved hearing improvement while on bevacizumab.[40,41]

The predictive power of our preclinical studies was corroborated by the clinical observation in the index patient, where the early transient tumor stabilization could also be explained by the rapid cell size reduction of NF2-deficient schwannoma cells in response to rapamycin, followed by progressive reduction of growth rate mirroring sirolimus blood concentrations. Moreover, rapid tumor volumetric growth following transient sirolimus withdrawal likely reflects a sudden increase in cell size, accompanied by cell cycle reentry and cell proliferation. Finally, upon reintroduction of

sirolimus, stabilization was immediately resumed, indicating that inhibition of mTORC1 had a direct inhibitory effect on VS growth, which therefore cannot be ascribed to the saltatory progression pattern described in the natural history of a rare subset of VS.[39,42] The observation that in this patient, a rapidly growing grade II meningioma did not respond to sirolimus therapy is likely explained by the fact that higher-grade meningiomas in NF2 patients carry chromosomal instability.[43] This can result in aberrant expression of cellular proliferative genes and silencing of other tumor suppressor genes, which can effectively modulate NF2-deficient tumor cell response to sirolimus.

Thus, the NF2 genetically engineered mouse schwannoma model appears to be predictive of treatment outcomes and strongly supports the application of the co-clinical trial concept in which mouse and human trials are conducted in parallel.[44–46] The encouraging and consistent result in an index patient, together with the preclinical results in mice, has now prompted phase II clinical trials to determine the efficacy of the rapalog everolimus for growing NF2 VS (clinicaltrials.gov: NCT01490476, NCT01345136, NCT01419639). The real challenge in the years to come will be to use targeted therapeutic modalities for effective NF2 tumor chemoprevention commensurate with an accurate estimate of drug safety and tolerability. This can be addressed by long-term treatment in genetically engineered mouse models and by clinical observations in cognate disease resulting in NF2 drug repurposing.

Supplementary Material

Supplementary material is available online at *Neuro-Oncology* (http://neuro-oncology.oxfordjournals.org/).

Funding

This work was supported in part by the Neurofibromatosis Preclinical Consortium, Children's Tumor Foundation; an Advocure NF2 Inc. award to M.G.; and the House Research Institute.

Acknowledgments

The authors thank Dr Mark Schwartz for providing surgical human NF2 tumor samples, and Benedicte Chareyre, Rosa Sierra, and Erica Canal for technical support. We thank Dr Zahara Jaffer for critical reading of the manuscript.

Conflict of interest statement. None declared.

References

1. Dolecek TA, Propp JM, Stroup NE, et al. CBTRUS statistical report: primary brain and central nervous system tumors diagnosed in the United States in 2005–2009. *Neuro Oncol*. 2012;14(Suppl 5):v1–v49.
2. Evans DG, Huson SM, Donnai D, et al. A clinical study of type 2 neurofibromatosis. *Q J Med*. 1992;84:603–618.
3. Blakeley JO, Evans DG, Adler J, et al. Consensus recommendations for current treatments and accelerating clinical trials for patients with neurofibromatosis type 2. *Am J Med Genet A*. 2012;158A:24–41.
4. Hadfield KD, Smith MJ, Urquhart JE, et al. Rates of loss of heterozygosity and mitotic recombination in NF2 schwannomas, sporadic vestibular schwannomas and schwannomatosis schwannomas. *Oncogene*. 2010;29:6216–6221.
5. Stemmer-Rachamimov AO, Xu L, Gonzalez-Agosti C, et al. Universal absence of merlin, but not other ERM family members, in schwannomas. *Am J Pathol*. 1997;151:1649–1654.
6. McClatchey AI, Fehon RG. Merlin and the ERM proteins—regulators of receptor distribution and signaling at the cell cortex. *Trends Cell Biol*. 2009;19:198–206.
7. Li W, Cooper J, Karajannis MA, et al. Merlin: a tumour suppressor with functions at the cell cortex and in the nucleus. *EMBO Rep*. 2012;13:204–215.
8. James MF, Han S, Polizzano C, et al. NF2/merlin is a novel negative regulator of mTOR complex 1, and activation of mTORC1 is associated with meningioma and schwannoma growth. *Mol Cell Biol*. 2009;29:4250–4261.
9. Lopez-Lago MA, Okada T, Murillo MM, et al. Loss of the tumor suppressor gene NF2, encoding merlin, constitutively activates integrin-dependent mTORC1 signaling. *Mol Cell Biol*. 2009;29:4235–4249.
10. Wong M. mTOR as a potential treatment target for epilepsy. *Future Neurol*. 2012;7:537–545.
11. Fingar DC, Salama S, Tsou C, et al. Mammalian cell size is controlled by mTOR and its downstream targets S6K1 and 4EBP1/eIF4E. *Genes Dev*. 2002;16:1472–1487.
12. Kwiatkowski DJ, Manning BD. Tuberous sclerosis: a GAP at the crossroads of multiple signaling pathways. *Human Mol Genet*. 2005;14(Spec No. 2):R251–R258.
13. Franz DN. Everolimus: an mTOR inhibitor for the treatment of tuberous sclerosis. *Expert Rev Anticancer Ther*. 2011;11:1181–1192.
14. Franz DN, Belousova E, Sparagana S, et al. Efficacy and safety of everolimus for subependymal giant cell astrocytomas associated with tuberous sclerosis complex (EXIST-1): a multicentre, randomised, placebo-controlled phase 3 trial. *Lancet*. 2013;381:125–132.
15. Kim DH, Sarbassov DD, Ali SM, et al. mTOR interacts with raptor to form a nutrient-sensitive complex that signals to the cell growth machinery. *Cell*. 2002;110:163–175.
16. Yip CK, Murata K, Walz T, et al. Structure of the human mTOR complex I and its implications for rapamycin inhibition. *Mol Cell*. 2010;38:768–774.
17. Phung TL, Ziv K, Dabydeen D, et al. Pathological angiogenesis is induced by sustained Akt signaling and inhibited by rapamycin. *Cancer Cell*. 2006;10:159–170.
18. Sarbassov DD, Ali SM, Sengupta S, et al. Prolonged rapamycin treatment inhibits mTORC2 assembly and Akt/PKB. *Mol Cell*. 2006;22:159–168.
19. Laplante M, Sabatini DM. mTOR signaling in growth control and disease. *Cell*. 2012;149:274–293.
20. James MF, Stivison E, Beauchamp R, et al. Regulation of mTOR complex 2 signaling in neurofibromatosis 2–deficient target cell types. *Mol Cancer Res*. 2012;10:649–659.
21. Giovannini M, Robanus-Maandag E, Niwa-Kawakita M, et al. Schwann cell hyperplasia and tumors in transgenic mice expressing a naturally occurring mutant NF2 protein. *Genes Dev*. 1999;13:978–986.
22. Yushkevich PA, Piven J, Hazlett HC, et al. User-guided 3D active contour segmentation of anatomical structures: significantly improved efficiency and reliability. *NeuroImage*. 2006;31:1116–1128.
23. Bashour AM, Meng JJ, Ip W, et al. The neurofibromatosis type 2 gene product, merlin, reverses the F-actin cytoskeletal defects in primary human schwannoma cells. *Mol Cell Biol*. 2002;22:1150–1157.
24. Pelton PD, Sherman LS, Rizvi TA, et al. Ruffling membrane, stress fiber, cell spreading and proliferation abnormalities in human Schwannoma cells. *Oncogene*. 1998;17:2195–2209.

25. Stemmer-Rachamimov AO, Louis DN, Nielsen GP, et al. Comparative pathology of nerve sheath tumors in mouse models and humans. *Cancer Res*. 2004;64:3718–3724.
26. Tanaka K, Eskin A, Chareyre F, et al. Therapeutic potential of HSP90 inhibition for neurofibromatosis type 2. *Clin Cancer Res*. 2013;19: 3856–3870.
27. Lee N, Woodrum CL, Nobil AM, et al. Rapamycin weekly maintenance dosing and the potential efficacy of combination sorafenib plus rapamycin but not atorvastatin or doxycycline in tuberous sclerosis preclinical models. *BMC Pharmacol*. 2009;9:8.
28. O'Reilly KE, Rojo F, She QB, et al. mTOR inhibition induces upstream receptor tyrosine kinase signaling and activates Akt. *Cancer Res*. 2006;66:1500–1508.
29. Bader AG, Kang S, Vogt PK. Cancer-specific mutations in PIK3CA are oncogenic in vivo. *Proc Natl Acad Sci U S A*. 2006;103:1475–1479.
30. Goudar RK, Shi Q, Hjelmeland MD, et al. Combination therapy of inhibitors of epidermal growth factor receptor/vascular endothelial growth factor receptor 2 (AEE788) and the mammalian target of rapamycin (RAD001) offers improved glioblastoma tumor growth inhibition. *Mol Cancer Ther*. 2005;4:101–112.
31. Nakamura H, Jokura H, Takahashi K, et al. Serial follow-up MR imaging after gamma knife radiosurgery for vestibular schwannoma. *Am J Neuroradiol*. 2000;21:1540–1546.
32. Choi H, Charnsangavej C, Faria SC, et al. Correlation of computed tomography and positron emission tomography in patients with metastatic gastrointestinal stromal tumor treated at a single institution with imatinib mesylate: proposal of new computed tomography response criteria. *J Clin Oncol*. 2007;25:1753–1759.
33. McClatchey AI, Giovannini M. Membrane organization and tumorigenesis—the NF2 tumor suppressor, Merlin. *Genes Dev*. 2005; 19:2265–2277.
34. Evans DG, Howard E, Giblin C, et al. Birth incidence and prevalence of tumor-prone syndromes: estimates from a UK family genetic register service. *Am J Med Genet A*. 2010;152A:327–332.
35. Evans DG, Kalamarides M, Hunter-Schaedle K, et al. Consensus recommendations to accelerate clinical trials for neurofibromatosis type 2. *Clin Cancer Res*. 2009;15:5032–5039.
36. Evans GR, Lloyd SK, Ramsden RT. Neurofibromatosis type 2. *Adv Otorhinolaryngol*. 2011;70:91–98.
37. Pachow D, Andrae N, Kliese N, et al. mTORC1 inhibitors suppress meningioma growth in mouse models. *Clin Cancer Res*. 2013;19: 1180–1189.
38. Mawrin C, Sasse T, Kirches E, et al. Different activation of mitogen-activated protein kinase and Akt signaling is associated with aggressive phenotype of human meningiomas. *Clin Cancer Res*. 2005;11:4074–4082.
39. Peyre M, Goutagny S, Bah A, et al. Conservative management of bilateral vestibular schwannomas in neurofibromatosis type 2 patients: hearing and tumor growth results. *Neurosurgery*. 2013;72: 907–914.
40. Mautner VF, Nguyen R, Kutta H, et al. Bevacizumab induces regression of vestibular schwannomas in patients with neurofibromatosis type 2. *Neuro Oncol*. 0000;12:14–18.
41. Plotkin SR, Stemmer-Rachamimov AO, Barker FG 2nd, et al. Hearing improvement after bevacizumab in patients with neurofibromatosis type 2. *N Engl J Med*. 2009;361:358–367.
42. Dirks MS, Butman JA, Kim HJ, et al. Long-term natural history of neurofibromatosis type 2–associated intracranial tumors. *J Neurosurg*. 2012;117:109–117.
43. Goutagny S, Bah AB, Henin D, et al. Long-term follow-up of 287 meningiomas in neurofibromatosis type 2 patients: clinical, radiological, and molecular features. *Neuro Oncol*. 2012;14: 1090–1096.
44. Chen Z, Cheng K, Walton Z, et al. A murine lung cancer co-clinical trial identifies genetic modifiers of therapeutic response. *Nature*. 2012; 483:613–617.
45. Lunardi A, Ala U, Epping MT, et al. A co-clinical approach identifies mechanisms and potential therapies for androgen deprivation resistance in prostate cancer. *Nat Genet*. 2013;45:747–755.
46. Nardella C, Lunardi A, Patnaik A, et al. The APL paradigm and the "co-clinical trial" project. *Cancer Disc*. 2011;1:108–116.
47. Rosen N, She QB. AKT and cancer—is it all mTOR? *Cancer Cell*. 2006;10: 254–256.